Propulsion and Power Research 2014;3(2):49–58

http://ppr.buaa.edu.cn/

Propulsion and Power Research

www.sciencedirect.com

ORIGINAL ARTICLE

Reynolds stress constrained large eddy simulation of separation flows in a U-duct

Quanyong Xu[a,b,*], Yantao Yang[b]

[a]*School of Aerospace, Tsinghua University, Beijing 100084, China*
[b]*Center for Applied Physics and Technology, College of Engineering, Peking University, Beijing 100871, China*

Received 27 June 2013; accepted 19 March 2014
Available online 26 June 2014

KEYWORDS

Reynolds stress constrain;
Large eddy simulation;
U-duct;
Separation;
Internal flow;
Computational fluid dynamics

Abstract This paper presents Reynolds stress constrained large eddy simulation (RSC-LES) method applied to a U-duct flow. Different from traditional Reynolds-averaged Navier-Stokes/ detached eddy simulation (RANS/DES) hybrid method (including DES method), the RSC-LES method solves the LES equations in the whole computation domain with the near-wall regions being constrained by a prescribed Reynolds stress. By doing so it is possible to overcome the log-law mismatch (LLM) problem in hybrid method. The RSC-LES results show better agreement with experiment result. Compared with RANS and DES, RSC-LES gives more accurate pressure coefficients and friction coefficients on the wall, because the RSC-LES method captures the separation point and reattachment point on the inner wall. The computation results show that the RSC-LES method has the potential to solve the log-law mismatch problem of RANS/DES hybrid method and predict complex phenomena of internal flow field.

*Corresponding author: Tel.: +86 10 62794843.
E-mail address: xuquanyong@tsinghua.edu.cn (Quanyong Xu).
Peer review under responsibility of National Laboratory for Aeronautics and Astronautics, China.

Production and hosting by Elsevier

1. Introduction

Computational fluid dynamics is playing an increasingly major role in the design and analysis of the internal flow in aeroengine components, such as inlet duct, compressor, combustor, etc. Most of these flows have complex features such as strong curvature, high turbulence levels, unsteadiness, and massive three-dimensional (3D) separation. Reynolds average Navier-Stokes (RANS) method fails to simulate separation flow correctly. Large eddy simulation

2212-540X
http://dx.doi.org/10.1016/j.jppr.2014.05.002

Nomenclature

H	channel height (unit: cm)
k	turbulence kinetic energy
L	shear stress of solved filter width (unit: Pa)
M	weighted coefficient of shear stress
p	pressure (unit: Pa)
Q	vortex criterion
R	Reynolds stress of scale be solved (unit: Pa)
S	deformation
s	dimensionless streamwise length
T	solved period (unit: s)
t	dimensionless time
U	streamwise velocity (unit: m/s)
u	velocity (unit: m/s)

Greek letters

ρ	density (unit: kg/m^3)
τ	shear stress of Δ filter width (unit: Pa)
Δ	filter width (unit: m)

Subscripts

i	x direction
j	y direction
mod	modeled parameter
S	Smargorinsky coefficient

(LES) shows great potential in these flow simulations, especially for unsteady flows with massive separations [1]. However, LES has its own challenges. For wall-bounded flows at high Reynolds number, pure LES is still far from affordable due to the huge requirement of computational resources [2]. One possible solution is using near-wall approximations [3,4], such as log-law or power-law functions. This allows a coarser near-wall resolution and remains an acceptable numerical accuracy in predicting flow properties.

In recent years, the hybrid RANS/LES methodology for wall-bounded flows has been developed and received increasing attention [5–9]. The hybrid RANS/LES approaches intend to combine the much lower near-wall resolution of RANS and higher accuracy of LES at outer region. In practice, the computation domain in a hybrid RANS/LES method is divided into RANS and LES regions explicitly. RANS-type equations based on certain turbulence model are solved within the inner layer. The solution will be used to generate the shear stress boundary conditions for LES in the outer layer. The rapid development of large-scale computers and the continuous improvement of the hybrid (or zonal) RANS/LES techniques have made the method popular to simulate engineering problems of interest [10–13]. Comprehensive discussion of the hybrid methods can be found in the review articles by Balaras & Benocci [14], Balaras et al. [15], Cabot [16], Cabot [17], Cabot & Moin [18], Piomelli & Balaras [19], Frohlich & von Terzi [20] and references therein. One of the most popular hybrid method is known as detached eddy simulation (DES), which was first proposed by Spalart et al. [21] based on the one-equation Spalart-Allmaras (S-A) model [22] to simulate the high Reynolds number turbulence with massive separations. DES uses a single turbulent model which automatically modifies the model equations according to a specific length scale. Initially, DES was designed to predict mean flow properties in the whole attached boundary layer by RANS, and to simulate the time-dependent large-scale motions in the shear layers and separated flow regions by LES. For more details of the DES formulation and its applications, readers are referred to Strelets [23], Piomelli & Balaras [24], and Spalart [25].

Despite their great successes in practical applications, hybrid RANS/LES methods remain problematic. One important issue is the discrepancy of the log-law intercepts between the RANS and the LES, characterized by an outward shift of the log-law profile (so called log-layer mismatch). This is believed to be associated with the appearance of a “super-buffer layer” near the RANS/LES interface [26,27]. As is well known, the resolved Reynolds stress shall contribute to the total shear stress dominantly in the outer LES region. In the RANS region, however, the flow field is smooth, and is characterized by the lack of realistic small-scale turbulence. The turbulent fluctuations, from which the Reynolds stresses are generated, cannot develop immediately at the RANS/LES interface to provide the “required” stresses. As a result, the resolved Reynolds stresses are underestimated in the transition zone, and the mean velocity gradient is steepened to compensate the low supply of the shear stresses. This also causes the “artificial” streaks and the underestimation of the skin-friction coefficient [26,28]. Solving this RANS/LES transition problem is an important step toward the overall success of the hybrid/zonal methods.

Many attempts have been made to eliminate the unphysical super-buffer layer and to improve the mean velocity profile for hybrid/zonal techniques. For instance, introducing an overlap zone was proven to be helpful to avoid the log-layer mismatch [29]. Some authors argue that the usage of backscatter models in the inner layer may also solve the transition problem [26,28]. Keating et al. [30] proposed to add controlled force together with synthetic turbulence at the interface in order to accelerate the generation of realistic turbulence near the transition region. These methods have achieved partial success. However, it appears that they are not general enough for different flow configurations. Recently, the improved delayed DES (IDDES) method [31] has been developed to solve this problem. Through the IDDES might not be the right direction in improving DES technique, since many empirical functions and constants are introduced in IDDES [25].

Using physical constraints on turbulence models was first proposed by Kraichnan in the constrained decimation theory [32]. In his approach, the effect of residual scales (subgrid scales) on the retained scales (large scales) is modeled by a stochastic forcing. To correctly calculate the mean energy flux, the forcing term is constrained to satisfy certain constraint equations deduced from underlying physics, such as symmetry and conservation. Kraichnan & Chen [33] extended the decimation idea to study intermittent phenomena by enforcing more constraints on high order statistics of fluid turbulence. The constraint idea has also been used by Ghosal et al. [34] to develop a dynamic localization SGS model by solving a variation problem under a nonnegative model coefficient constraint. Meneveau [35] suggested a series of balance conditions in the LES, which are supposed to predict the turbulence statistics accurately when modeling the subgrid-scale (SGS) stress. Recently, a dynamic SGS model with an energy dissipation constraint has been developed by Shi et al. [36]. It is found that the constrained SGS (C-SGS) model not only predicts the turbulent dissipation accurately, but also shows a strong correlation with the real stress from a priori test, which is a desirable feature combining the advantages of dynamic Smagorinsky and mixed models. The C-SGS models, from both a priori and a posteriori tests, improve other features in the dynamic mixed models, including ability to reproduce the probability density distribution of subgrid stresses and the energy backscatter.

Encouraged by the above works, this paper applies a new constrained LES model for wall-bounded turbulence [37]. In this approach, the entire flow region is solved through LES, while a Reynolds stress constraint (RSC) is enforced on the SGS model in the inner layer to ensure that a prescribed Reynolds stress condition is satisfied. The underlying dynamics, is consistent with the balance condition by Meneveau [35] and the coupling equations. The philosophy of the Reynolds stress constrained large eddy simulation (RSC-LES) is fundamentally different from the hybrid RANS-LES approaches. The starting point of RSC-LES is that the LES naturally includes the small-scale fluctuations in the whole flow domain. The RANS equations do not need to be solved in the inner layer (called constrained LES region) for RSC-LES, but the mean velocity of the inner layer flow field predicted by the RSCSGS model satisfies the RANS equations automatically. The Reynolds stress constraint is uninstalled from the SGS model from the bottom of the outer layer (called non-constrained region). As discussed above, the most important thing to remove the super-buffer layer near the RANS/LES interface is to allow a smooth transition of the small-scale fluctuations. That is indeed the case for RSC-LES. We want to stress here that RSC-LES only needs to employ the same grid resolution as used in DES. In simulation of the channel flow, the total number of grids required by DES (as well as RSC-LES) is simply proportional to the wall Reynolds number [27]. In a sharp contrast, traditional LES needs a number proportional to $Re^{1.8}$ to solve the inner layer flow [24], which is much more expensive than DES and RSC-LES.

In this paper, RSC-LES is adopted to simulate separation flows. The RSC-LES solves uniform LES equations in the whole flow field. The near wall small-scale fluctuations are generated by LES calculating results. In order to reduce near wall grid number, RSC-LES introduces additional Reynolds stress to constrain the average velocity at near-wall regions. Therefore RSC-LES can use coarse grids as RANS/LES hybrid methods or DES methods. So the RSC-LES method can solve LLM problem inherently and take affordable computation costs.

2. RSC-LES methodology

In this paper we utilize a new Reynolds stress constrained LES model for u-duct flow simulation. In our approach, the entire flow region is solved through LES equation, while a Reynolds stress constraint is enforced on the SGS model in the inner layer to ensure that a prescribed Reynolds stress condition is satisfied. The details of the RSC-LES model have been reported in reference [37], here we only give a brief description for completeness.

In this paper, the flow Mach number in the duct flow is about 0.1 [38]. Thus we use incompressible low-pass filtered Navier-Stokes equations to solve the large scales flow, which read:

$$\frac{\partial \widetilde{u}_i}{\partial x_i} = 0 \tag{1}$$

$$\frac{\partial \widetilde{u}_i}{\partial t} + \frac{\partial (\widetilde{u}_i \widetilde{u}_j)}{\partial x_j} = -\frac{1}{\rho}\frac{\partial (\widetilde{p})}{\partial x_i} + \upsilon \frac{\partial^2 \widetilde{u}_i}{\partial x_j \partial x_j} - \frac{\partial \tau_{ij}}{\partial x_j} \tag{2}$$

Here, a tilde denotes low-pass filtering with a filter width Δ is the large-scale velocity, $\widetilde{p}$ is the filtered pressure and υ is the kinetic viscosity, respectively. The large-scale motions are resolved directly, while the small-scale effects on the large scale dynamics are modeled through the subgrid stress:

$$\tau_{ij} = \widetilde{u_i u_j} - \widetilde{u}_i \widetilde{u}_j \tag{3}$$

At outer region, the deviatoric components of SGS stress (1.3) are modeled by dynamic Smargorinsky SGS model [39,40], as

$$\tau_{ij}^{mod} = C_s \Delta^2 \left|\widetilde{S}\right| \widetilde{S}_{ij} \tag{4}$$

$$C_s = \frac{\langle L_{ij} M_{ij} \rangle}{\langle M_{ij} M_{ij} \rangle} \tag{5}$$

$$M_{ij} = (2\Delta)^2 \overline{\left|\widetilde{S}\right|}\, \overline{\widetilde{S}}_{ij} - \Delta^2 \overline{\left|\widetilde{S}\right| \widetilde{S}_{ij}} \tag{6}$$

$$L_{ij} = \overline{\widetilde{u}_i \widetilde{u}_j} - \overline{\widetilde{u}_i}\, \overline{\widetilde{u}_j} \tag{7}$$

where a bar means filtering at subtest scale 2Δ.

At inner region, we enforce constrain on the modeled shear stress, as

$$\tau_{ij}^{mod} = R_{ij}^{mod} - R_{ij}^{LES} - C_s'(\Delta^2 \left|\widetilde{S}\right| \widetilde{S}_{ij} - \langle \Delta^2 \left|\widetilde{S}\right| \widetilde{S}_{ij} \rangle) \quad (8)$$

Here,

$$R_{ij}^{mod} = -2\upsilon_T \langle \widetilde{S}_{ij} \rangle \quad (9)$$

$$R_{ij}^{LES} = \langle \widetilde{u}_i \widetilde{u}_j \rangle - \langle \widetilde{u}_i \rangle \langle \widetilde{u}_j \rangle \quad (10)$$

$$C_s = \frac{\langle L'_{ij} M'_{ij} \rangle}{\langle M'_{ij} M'_{ij} \rangle} \quad (11)$$

The angle bracket above denotes the mean of spanwise average. Detail derivation can be referred in [41]. The interface between inner and outer regions should be located in the place where small-scale fluctuations have been full development. In this paper, we use the modified distance function recommended by Spalart [21] as the interface distance away from wall.

3. U-duct experiment condition

The U-duct experiment case is carried out by NASA to evaluate new turbulence model for strong-curved internal flows [37]. The low speed internal flow in a 180° bend U-duct has been conducted. The flow contains all of the complex features often occurring in engine flows as mentioned before. The test conditions referred in this paper are listed in Table 1.

The U-duct configuration is shown in Figure 1. The turn has an inner radius of 1.91 cm and an outer radius of 5.72 cm. The computing domain extends from $x/H = -4$ upstream of the bend to $x/H = 12$ downstream. In order to compare with the experiment results, the computing domain extends from $z/H = 0$ to $z/H = 4$ in the spanwise direction.

Table 1 U-duct experiment parameters.

Test condition	Value
Channel height, H/cm	3.81
Inlet velocity, U_b/(m/s)	31.1
Reynolds number based on H and U_b	1×10^6
Aspect ratio, B/H	10
Test temperature/°C	−9
Inlet Mach number	0.1

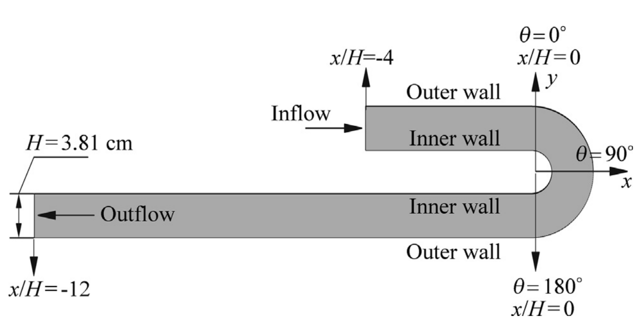

Figure 1 U-duct flow domain configuration.

4. Numerical approaches

The numerical calculations were carried out using a validated finite volume algorithm Fluent with a user-defined-function (UDF) code to solve the incompressible LES Eqs. (1) and (2). The pressure-based solver utilizes a SIMPLE scheme to discrete the governing equations. The spatial discretization uses second order upwind scheme,

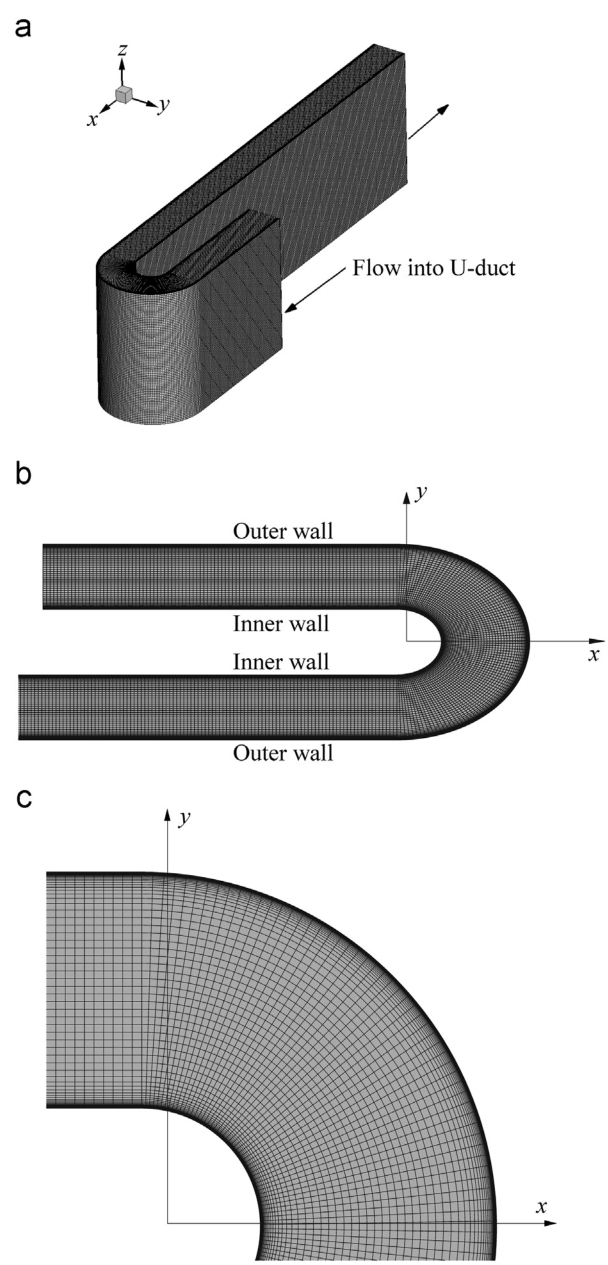

Figure 2 U-duct grids. (a) The whole flow field grid, (b) the top view, and (c) the bent segment enlargement view.

and the temporal discretization uses second order implicit scheme. Based on a dynamic Smagorinsky-Lilly SGS model, the RSC-LES method adds the new stress terms of Eq. (8).

The finest resolution is 500 in $\times$ 80 in $\times$ 80 in the streamwise, normal and spanwise directions respectively. The minimum normal spacing at the wall is 1.0×10^{-5} m, which yields an average y^+ value around 1.0. The simulation has also been done with coarser grids and minor mesh-dependent was found. For comparison we also report the results obtained by the RANS method with Spalart-Allmaras one equation turbulence model [22] and the delayed DES [42] with Spalart-Allmaras model for RANS/LES hybrid mthod.

As for the boundary condition, we use the u-velocity profile measured by experiment at inlet, constant statis pressure at outlet, and periodic condition at the spanwise direction. All the walls are non-slip (Figure 2).

5. Results and discussion

The wall static pressure coefficients (C_p) are plotted in Figure 4. The abscissa represents the curve length along the duct centerline. In order to keep consistent with the experimental data, the range of s is from 17.67 to 36.81. In the following we divide the duct into three part: a) the upstream segment with $17.67 < s < 21.67$, b) the bend segment with $21.67 < s < 24.81$, and c) the downstream segment with $24.81 < s < 36.81$. In the upstream segment, the flow is fully developed turbulent but without massive separation. Thus the traditionl RANS and DES are able to capture the C_p correctly as our new RSC-LES model.

In the bend segment, massive separation emerges and the flow characteristics are total different near the inner and outer walls. In the first half of the bend segment ($21.67 < s < 23.24$), the pressure drops along the inner wall as the flow accelerates, and rises on the outer wall as the

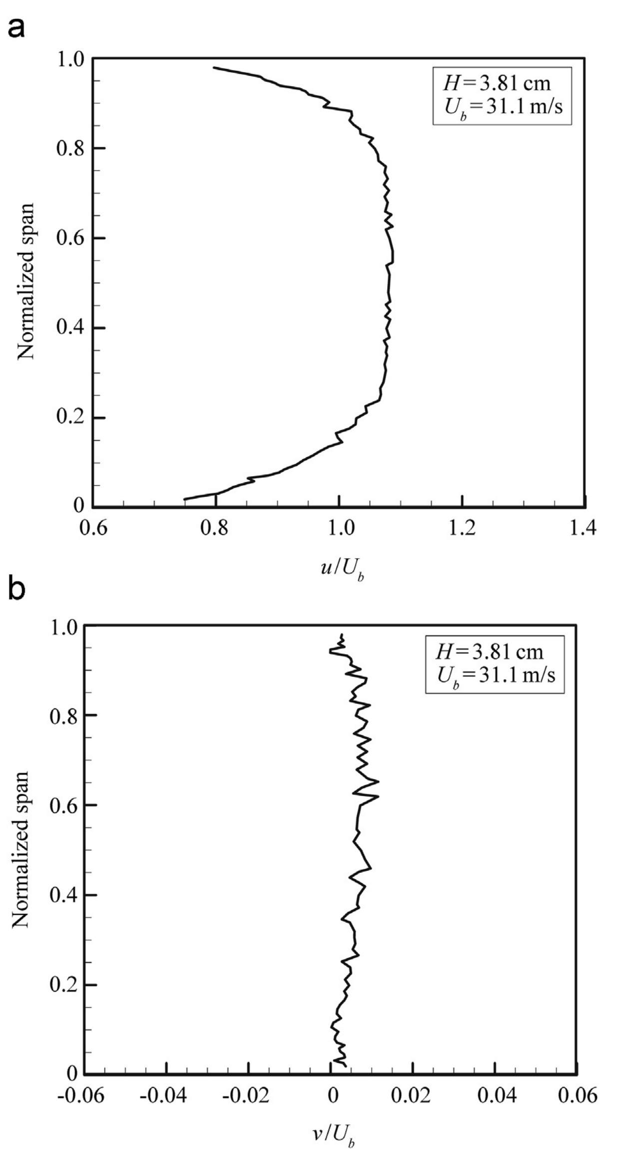

Figure 3 Inlet boundary velocity profile. (a) Streamwise velocity and (b) normal velocity.

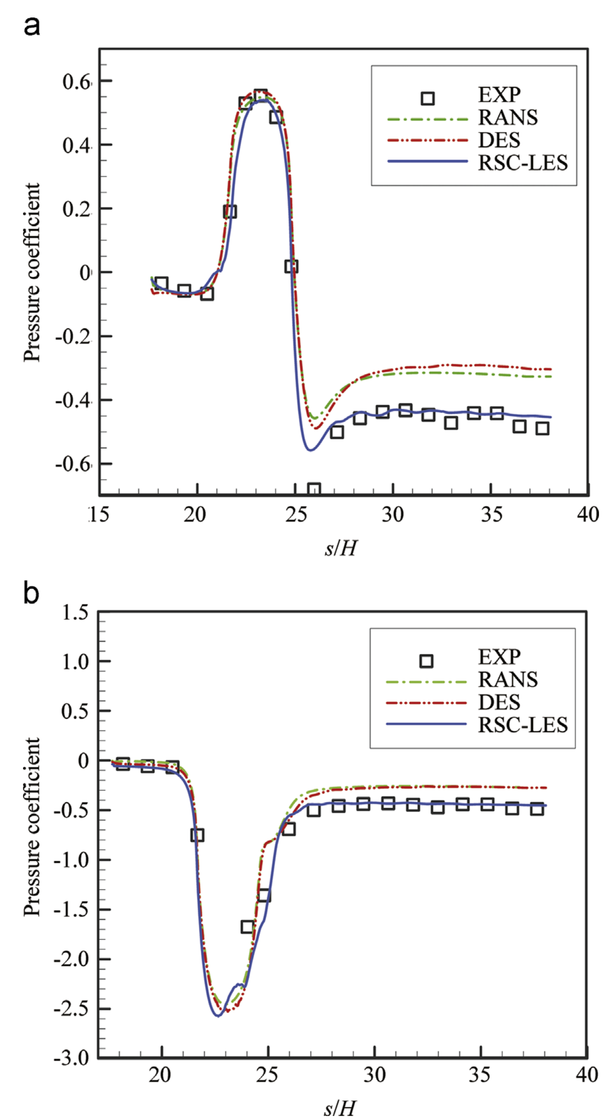

Figure 4 Wall static pressure coefficients distributions. (a) Inner wall and (b) outer wall.

flow there decelerates. In the second half of the bend segment ($23.24<s<24.81$), the opposite effects occur, leading to the separation of the boundary on the inner wall.

In the downstream segment, C_p is lower than that at the upstream segment. This pressure drop represents the dissipation losses in the flow caused by the presence of the bend. Compared with the experiment data, C_p obtained by RSC-LES agrees better than that of RANS, and DES results. This implies that the RSC-LES method predicts the turbulent dissipation more accurate than RANS and DES. The flow separates and strong mixing happens here. RANS and DES overestimate the dissipation and therefore produce higher static pressure than the experiment value.

In Figure 5, we plot the wall friction coefficient C_f on the inner wall rises steeply in the first half of the bend segment as the flow accelerates. The RSC-LES results predict closest than RANS and DES result. Near the end of the bend segment, the inner wall C_f plunges steeply to the negative values because the flow separates. At separation point and reattachment point, C_f on the inner wall equals zero and change sign, this can be used to identify the separation zone. The RANS and DES can't capture the separation point accurately. In the downstream segment, the inner wall C_f distributions recover and overshoot their up stream values before relaxing back to those levels. It is because RANS and DES predict the dissipation accurately. Figure 6 illustrates that the turbulence kinetic energy predicted by the RANS and DES are much lower than that by RSC-LES at 180 degree of the bend. This result indicates that the RSC-LES predicts small-scale fluctuations more accurately near the wall.

The flow in the whole computing region is turbulent. At the inlet the flow has fully-turbulent boundary layers with the thickness of about $0.25H$ on the inner and outer walls, as shown in Figure 3. The streamwise velocity profile is symmetric about the center line.

In the first half of the bend, the flow accelerates near the inner wall and decelerates near the outer wall, which makes the streamwise velocity profile very asymmetric at the 0 degree position of the bend, as show in Figure 7(a). The asymmetry becomes more obvious at the 90 degree position of the bend, as show in Figure 7(b). It is affected by convex curvature of the inner wall, and concave curvature of the outer wall.

In the second half of the bend segment, the flow decelerates near the inner wall and accelerates near the outer wall. The flow separates on the inner wall at the 150 degree of the bend, and reattaches at $x/H=1.5$. Strong mixing appears due to the flow separation. The asymmetry

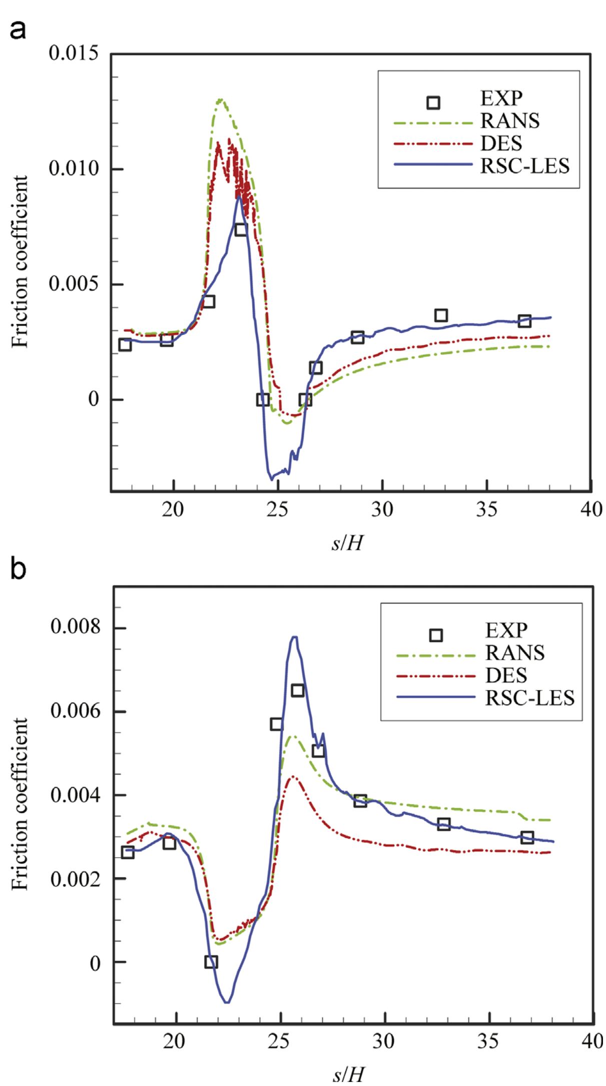

Figure 5 Wall friction coefficients distributions. (a) Inner wall and (b) outer wall.

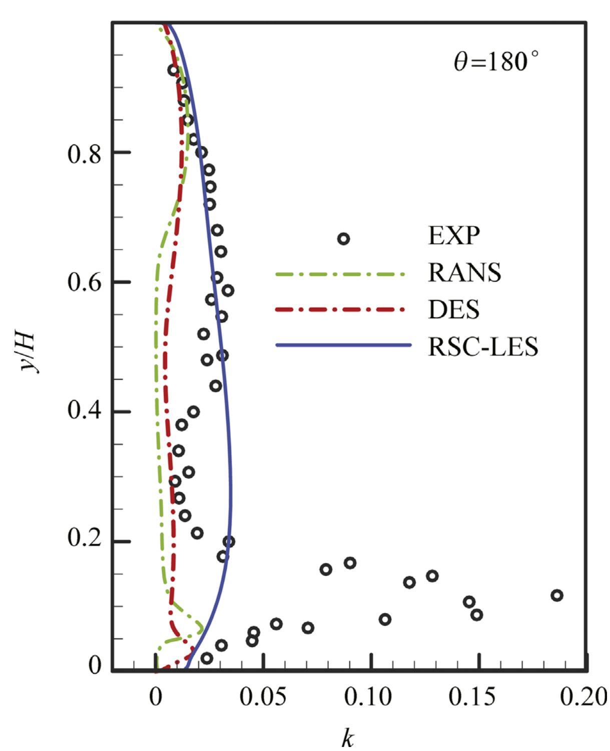

Figure 6 Turbulence kinetic energy profile at 180 degree of the bend.

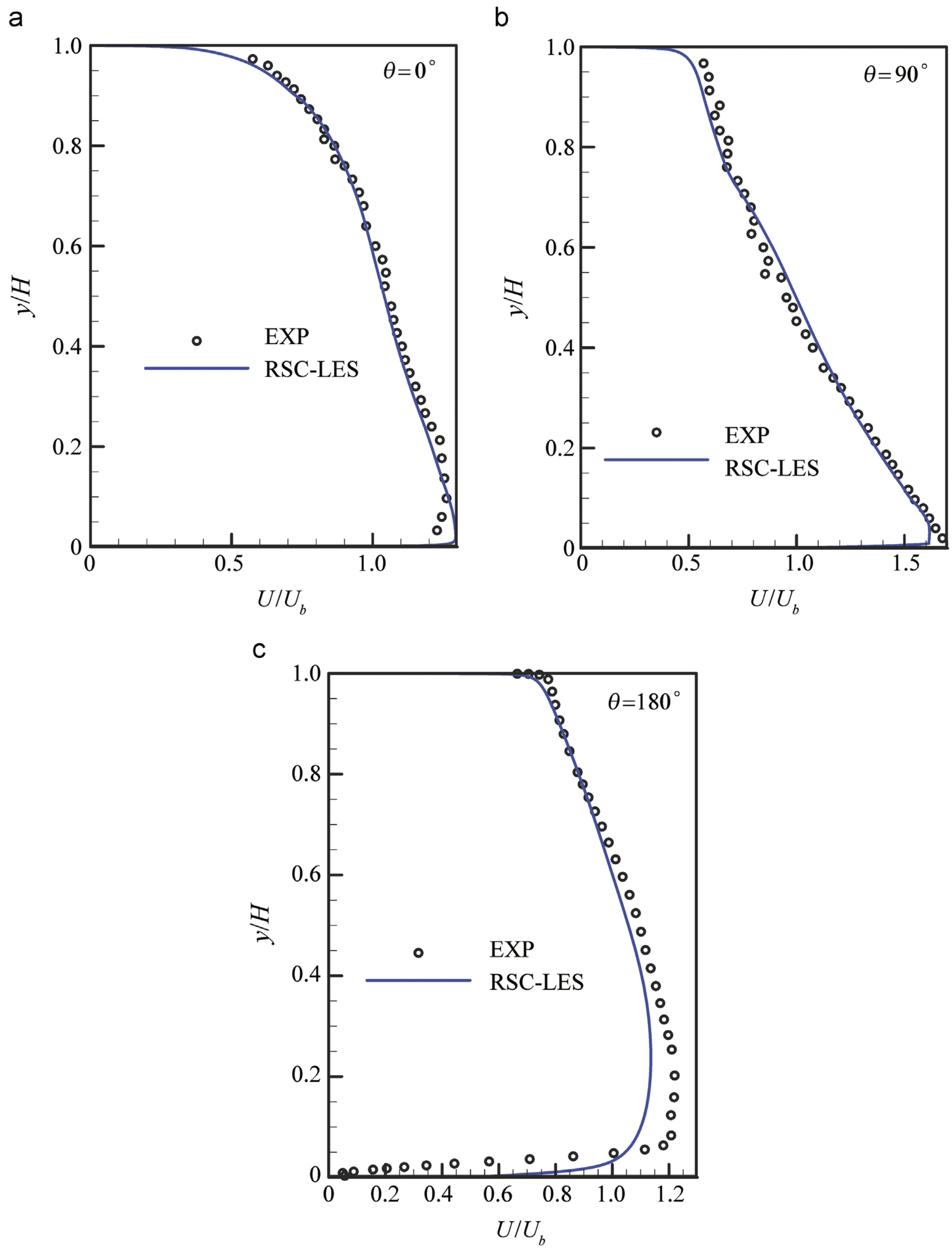

Figure 7 Streamwise velocity profile comparison. (a) 0 degree of the bend, (b) 90 degree of the bend, and (c) 180 degree of the bend.

of the streamwise velocity profile weakens as the flow exit the bend segment, as shown in Figure 7(c).

The inaccurate fluctuation prediction below 20% height of the span (in Figure 6) results in bad mean velocity results near the inner wall (shown in Figure 7(c)). The streamwise velocity near the inner wall is smaller than the experiment data at the 180 degree of the bend. Because there is a separation zone near the inner wall. The velocity profiles given by RSC-LES method do not agree so well as that at 0 degree and 90 degree position. But still it is higher than RANS and DES.

Figure 8 presents the reparation zones near outer wall upstream and inner wall downstream of the bend segment. As mentioned above, the pressure rises on the outer wall as the flow there decelerates in the first half of the bend.

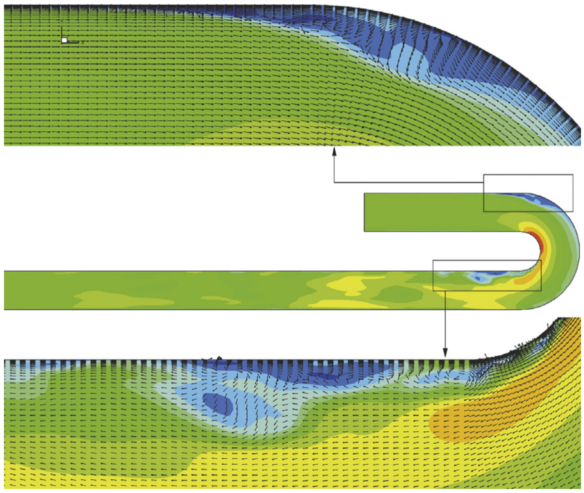

Figure 8 Instantaneous velocity of U-duct with separation zones.

And also the pressure rises at the second half of the bend near the inner wall. So the two separation zones are all caused by the adverse pressure gradient. The flow will reattach on the wall when the pressure gradient drops down. The wall friction coefficient equals zero at the separation point and reattached point, as shown in Figure 5.

Figure 9 shows the times instantaneous vertex structures depicted by Q-criterion at four different time steps. The color of the vortices in Figure 9 represents the velocity magnitude. The vortices generate from the outer wall upstream and inner wall down stream, near the separation zones. The vortices generated from the outer wall have larger scale than that from the inner wall. The outer vortices move downstream with the flow until interacting with the inner wall vortices. From (1/4)T to (4/4)T, it is found that the outer wall vortices intermittently eject up and sweep down. Those large scale vortices immediately mix with the vortices from the inner wall and spread to the entire channel. At the outlet of the flow field, the velocity of the flow blends by the vortex mixing.

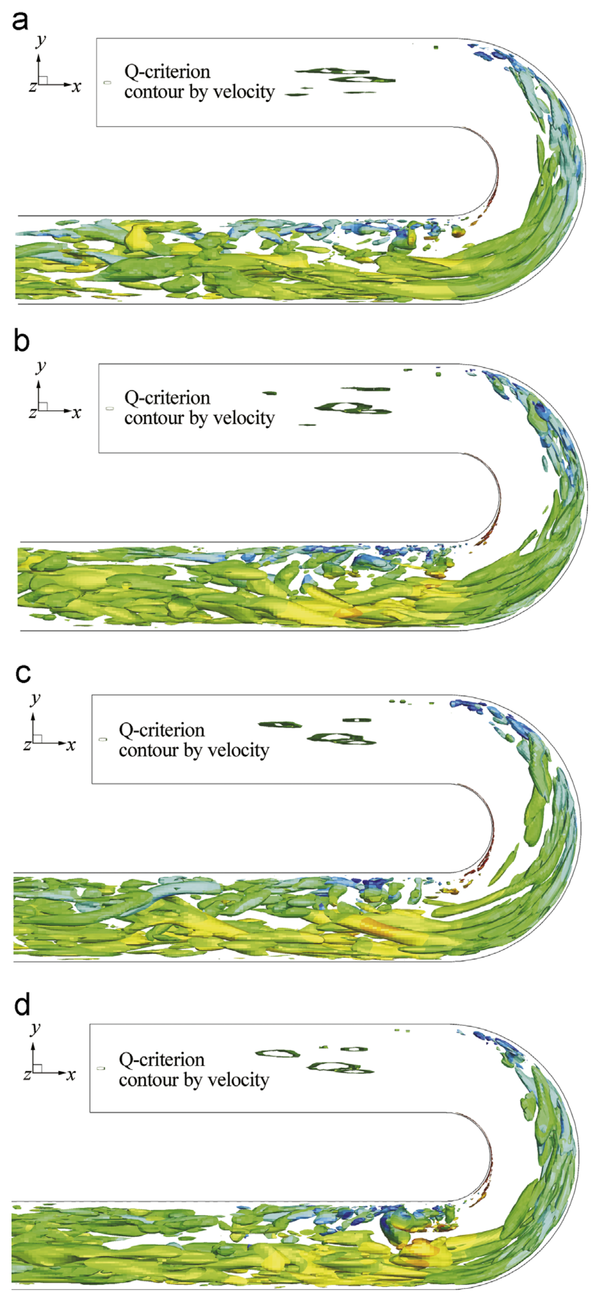

Figure 9 Instantaneous vortex structure by Q-criterion. (a) $t=(1/4)T$, (b) $t=(2/4)T$, (c) $t=(3/4)T$, and (d) $t=(4/4)T$.

6. Conclusion

This paper presents Reynolds stress constrained large eddy simulation (RSC-LES) method applied to a U-duct flow. Different from traditional RANS/DES hybrid method (including DES), the RSC-LES method solves the LES equations in the whole computation domain with the near-wall regions being constrained by a prescribed Reynolds stress. By doing so it is possible to overcome the log-law mismatch problem in hybrid method. The RSC-LES results show better agreement with experiment result. Compared with RANS and DES, RSC-LES gives more accurate pressure coefficients and friction coefficients on the wall, because the present method captures the separation point and reattachment point on the inner wall. In the separation zone the velocity profiles exhibit minor discrepancy with the experiment, this may attribute to the RANS constrained approach. It is worthy to investigate other constrained approach. Nevertheless, the RSC-LES results show strong capacity to simulate high Reynolds number, separated internal flows with less grid points, and give better results than DES or other RANS/LES hybrid methods.

References

[1] N.J. Georgiadis, Introduction: large-eddy simulation current capabilities and areas of needed research, Progress in Aerospace Sciences 44 (2008) 379–380.

[2] U. Piomelli, E. Balaras, Wall-layer models for large-eddy simulations, Annual Review of Fluid Mechanics 34 (2002) 349–374.
[3] J.W. Deardorff, A numerical study of three-dimensional turbulent channel flow at large Reynolds numbers, Journal of Fluid Mechanics 41 (1970) 453–480.
[4] U. Schumann, Subgrid scale model for finite difference simulations of turbulent flows in plane channels and annuli, Journal of Computational Physics 18 (1975) 376–404.
[5] P.R. Spalart, Strategies for turbulence modeling and simulations, International Journal of Heat and Fluid Flow 21 (2000) 252–263.
[6] A. Dejoan, R. Schiestel, LES of unsteady turbulence via a one-equation subgrid-scale transport model, International Journal of Heat and Fluid Flow 23 (2002) 398–412.
[7] L. Davidson, S.H. Peng, Hybrid LES-RANS modeling: a one-equation SGS model combined with a $k-\omega$ model for predicting recirculating flows, International Journal for Numerical Methods in Fluids 43 (2003) 1003–1018.
[8] F. Tessicini, L. Temmerman, M.A. Leschziner, Approximate near-wall treatments based on zonal and hybrid RANS/LES methods for LES at high Reynolds numbers, International Journal of Heat and Fluid Flow 27 (2006) 789–799.
[9] P. Sagaut, S. Deck, M. Terracol, Multiscale and Multiresolution Approaches in Turbulence, Imperial College Press, London, 2006.
[10] M. Shur, P.R. Spalart, M. Strelets, A. Travin, Detached-eddy simulation of an airfoil at high angle of attack, in: W. Rodi, D. Laurence (Eds.), The Fourth International Symposium on Engineering Turbulence Modeling and Experiments, Corsica, Elsevier, New York, 1999.
[11] E. Labourasse, P. Sagaut, Reconstruction of turbulent fluctuations using a hybrid RANS/LES approach, Journal of Computational Physics 182 (2002) 301–336.
[12] S. Kapadia, S. Roy, Detached eddy simulation over a reference ahmed car model, in: The 41th AIAA Aerospace Sciences Meeting and Exhibit, Reno, NV, AIAA-2003–0857, 2003.
[13] K.D. Squires, Invited lecture: detached-eddy simulation: current status and perspectives, ERCOFTAC Series 9 (2004) 465–480.
[14] E. Balaras, C. Benocci, Subgrid-scale models in finite-difference simulations of complex wall bounded flows, In: AGARD, pp. 2.1-2.5, France, AGARD: Neuilly-Sur-Seine, 1994.
[15] E. Balaras, C. Benocci, U. Piomelli, Two-layer approximate boundary conditions for large-eddy simulations, AIAA Journal 34 (1996) 1111–1119.
[16] W.H. Cabot, Large-eddy simulations with wall models, in: Annual Research Briefs, Stanford University, Center for Turbulence Research, 1995, pp. 41-50.
[17] W.H. Cabot, Near-wall models in large eddy simulations of flow behind a backwardfacing step, in: Annual Research Briefs, Stanford University, Center for Turbulence Research, 1996, pp. 199-210.
[18] W.H. Cabot, P. Moin, Approximate wall boundary conditions in the large-eddy simulation of high Reynolds number flows, Flow, Turbulence and Combustion 63 (1999) 269–291.
[19] U. Piomelli, E. Balaras, Wall-layer models for large-eddy simulations, Annual Review of Fluid Mechanics 34 (2002) 349–374.
[20] J. Frohlich, von D. Terzi, Hybrid LES/RANS methods for the simulation of turbulent flows, Progress in Aerospace Sciences 44 (2008) 349–377.
[21] P.R. Spalart, W.H. Jou, M. Strelets, S.R. Allmaras, Comments on the feasibility of LES for wings and on a hybrid RANS/LES approach, in: Advances in DNS/LES, Greyden Press, Columbus, OH, 1997, pp. 137-148.
[22] P.R. Spalart, S.R. Allmaras, A one-equation turbulence model for aerodynamic flows, Research Aerospace 1 (1994) 5–21.
[23] M. Strelets, Detached-eddy simulation of massively separated flows, in: American Institute of Aeronautics & Astronautics, Washington, DC, AIAA-2001–0879, 2001.
[24] U. Piomelli, E. Balaras, Wall-layer models for large-eddy simulations, Annual Review of Fluid Mechanics 34 (2002) 349–374.
[25] P.R. Spalart, Detached-eddy simulation, Annual Review of Fluid Mechanics 41 (2009) 181–202.
[26] J.S. Baggett, On the feasibility of merging LES with RANS in the near-wall region of attached turbulent flows, in: Annual Research Briefs, Stanford University, Center for Turbulence Research, 1998, pp. 267-277.
[27] N.V. Nikitin, F. Nicoud, B. Wasistho, K.D. Squires, P.R. Spalart, An approach to wall modeling in large-eddy simulations, Physics of Fluids 12 (2000) 1629–1632.
[28] U. Piomelli, E. Balaras, H. Pasinato, K.D. Squires, P.R. Spalart, The inner-outer layer interface in large-eddy simulations with wall-layer models, International Journal of Heat and Fluid Flow 24 (2003) 538–550.
[29] F. Hamba, An approach to hybrid RANS/LES calculation of channel flows, in: Engineering Turbulence Modelling and Experiments, Elsevier, Amsterdam, 5 (2002) 297–306.
[30] A. Keating, G. de Prisco, U. Piomelli, Interface conditions for hybrid RANS/LES calculations, International Journal of Heat and Fluid Flow 27 (2006) 777–788.
[31] M. Shur, P.R. Spalart, M. Strelets, A. Travin, A hybrid RANS-LES approach with delayed-DES and wall-modelled LES capabilities, International Journal of Heat and Fluid Flow 29 (2008) 1638–1649.
[32] R.H. Kraichnan, Theoretical approaches to turbulence, in: Applied Mathematical Sciences Series, Springer-Verlag, 58 (1985) 91.
[33] R.H. Kraichnan, S. Chen, Is there a statistical mechanics of turbulence?, Physica D: Nonlinear Phenomena 37 (1989) 160–172.
[34] S. Ghosal, T.S. Lund, P. Moin, K. Akselvoll, A dynamic localization model for large-eddy simulation of turbulent flows, Journal of Fluid Mechanics 286 (1995) 229–255.
[35] C. Meneveau, Statistics of turbulence subgrid-scale stresses: Necessary conditions and experimental tests, Physics of Fluids 6 (1994) 815–833.
[36] Y.P. Shi, Z.L. Xiao, S.Y. Chen, Constrained subgrid-scale stress model for large eddy simulation, Physics of Fluids 20 (2008) 011701.
[37] S.Y. Chen, Z.H. Xia, S.Y. Pei, J.C. Wang, Y.T. Yang, Z.L. Xiao, Y.P. Shi, Reynolds-stress-constrained large eddy simulation of wall bounded turbulent flows, Journal of Fluid Mechanics 703 (2012) 1–28.
[38] J.M. Daryl, H.L. Seegmiller, An experimental investigation of subsonic flow in a two-dimensional U-duct, NASA Technical Memorandum 103931 (1992).

[39] D.K. Lilly, A proposed modification of germano subgrid-scale closure method, Physics of Fluids A: Fluid Dynamics 4 (1992) 633–635.

[40] C. Meneveau, J. Katz, Scale-invariance and turbulence models for large-eddy simulation, Annual Review of Fluid Mechanics 32 (2000) 1–32.

[41] S. Pei, Reynolds stress constrained large-eddy simulation method and its simulation for turbulent channel flow, MS dissertation, Peking University, Beijing, 2008.

[42] P.R. Spalart, S. Deck, M.L. Shur, K.D. Squires, M.Kh. Strelets, A. Travin, A new version of detached-eddy simulation, resistant to ambiguous grid densities, Theoretical and Computational Fluid Dynamics 20 (2006) 181–195.